Finite Element Modeling of Heat Transfer in Carbon-Carbon Composites

J. W. Klett[1], V. J. Ervin[2], D. D. Edie[3]

[1]Carbon and Insulation Materials Technology Group, Metals and Ceramics Division,
Oak Ridge National Laboratory, Oak Ridge, TN, 37831-6087

[2]Department of Mathematical Sciences, Clemson University, Clemson, SC, USA, 29634

[3]Department of Chemical Engineering and Center for Advanced Engineering Fibers,
Clemson University, Clemson, SC, USA, 29634

Abstract - A finite element model was developed to predict the thermal conductivity, both parallel and transverse to the fiber axis, of unidirectional carbon-carbon composites. This versatile model incorporates fiber morphology, matrix morphology, fiber/matrix bonding, and random distribution of fibers, porosity, and cracks. The model first examines the effects of the preceding variables on the thermal conductivity at the microscopic level and then utilizes those results to determine the overall thermal conductivity. The model was able to accurately predict the average thermal conductivity of standard pitch-based carbon-carbon composites.

The model was also used to study the effect of different composite architectures on the bulk thermal conductivity. The effects of fiber morphology, fiber/matrix interface, and the ratio of transverse fiber conductivity to matrix conductivity on the overall composite conductivity was examined.

Key Words - carbon-carbon, mesophase, thermal conductivity, finite element, modeling

1. INTRODUCTION

Over the last several decades, computer modeling has become a powerful tool for the engineering analysis of complex systems. In today's "high-tech" aerospace industry, finite element modeling is used extensively to predict the behavior of materials at severe conditions. For instance, the proposed shuttle replacement, VentureStar, will require carbon-carbon protective shields that can withstand a temperature change from -50°C to 2000°C in a matter of minutes. Unfortunately, the experimental equipment which could simulate this variation (and the related environment) is extremely expensive. Therefore, computer-based numerical models are being developed to predict the thermal transport properties of these composite heat shields. The objective is to determine the necessary composite thickness, fiber architecture, and composite shape which yields the maximum thermal efficiency and meets vehicle weight constraints.

Therefore, a major goal of the present research was to develop a model which will yield insight into the thermal transport properties of carbon-carbon composites, both perpendicular and parallel to the fiber axis. Since carbon-carbon is a three-phase, anisotropic, heterogeneous material, developing a rigorous model would be virtually impossible. In recent years several attempts have been made to model material constants for composites and continues to be an active area of research. They have been primarily based upon Ohm's Law[1,2], variable dispersion models[3-7], estimations based upon calculations for a fundamental unit[6,8], and homogenization concepts[9,10]. However, these models do not account for all the variables that influence the thermal properties of carbon-carbon (fiber and matrix anisotropy, random distribution of fibers, cracks, and voids, etc.). Therefore, the current research focused on developing a comprehensive model which can account for the many different variables that influence the thermal conductivity of carbon-carbon.

2. DEFINITION OF PROBLEM

The objective of the mathematical model is to predict the rather complex thermal transport properties of carbon-carbon composites (illustrated in Figure 1). Figure 1(a) is a section (transverse to the fiber axis) of a carbon-carbon composite formed from a polymeric matrix precursor (PEEK) and AS-4 PAN-based carbon-fibers. In this direction, both the matrix and the fibers have a random microstructure, leading to locally isotropic material properties in the heterogeneous material. On the other hand, Figure 1(b) shows a transverse section of a carbon-carbon composite formed from a pitch matrix precursor and pitch-based P55 fibers. Here, both the matrix and the fibers are highly anisotropic. Both figures represent typical carbon-carbon composites. Therefore, any comprehensive model must be able to account for these drastically different structures.

Numerous variables must be accounted for if the model is to be comprehensive. To begin with, the model must account for the random distribution of fibers, microscopic cracks and large voids throughout the composite. In addition, the individual fibers can have either a highly ordered microstructure or a fairly random microstructure. The matrix can be relatively isotropic or it can be highly anisotropic (i.e., the matrix orients in a sheath-like structure around the fiber). Last, the fiber/matrix interface can be well developed or poorly developed (i.e. the matrix debonds from the fibers).

In the following sections a finite element model will be developed in which the local thermal properties of a single fiber and its surrounding matrix are studied on the microscopic level both transverse and parallel to the fiber axis. Furthermore, the effects of microscopic cracks in the matrix and fiber/matrix debonding will be included at this point. Then a model is developed to study the thermal properties of a composite on the macroscopic level by both using

the information learned on the microscopic level and incorporating the effects of macroscopic voids (e.g. porosity).

Finally, the versatility of the model is shown by utilizing it to isolate the effects of several material characteristics on the overall thermal conductivity. For instance, a basic understanding of the effects of the fiber properties on transverse thermal conductivity is important to the designer so wasted energy is not spent on a design condsideration that is not significant.

The authors recognize that the thermal conductivity of carbon-carbon is dependent on temperature amd that the materials studied will most likely be used in environments where extreme temperatures are present. However, the temperature dependence of carbons is will characterized and not the focus of this work and thus the prediction of steady state thermal conductivity at room temperature is addressed. Perhaps in future work the model developed here can be modified to include both temperature dependence of thermal conductivity and the thermal expansion properties (which will affect the size and shape of microcracks). Hence, the model derivation follows.

Under steady state conditions, no heat source, and Fourier's Law of heat conduction are assumed, the Equation of Energy for heat transfer in a solid can be reduced to the following over a given region Ω in the composite:

$$\iint_{\Omega} \vec{\nabla} \cdot \bar{q} \, d\Omega = \iint_{\Omega} \vec{\nabla} \cdot \begin{bmatrix} \kappa_x & 0 \\ 0 & \kappa_y \end{bmatrix} \vec{\nabla} T \, d\Omega = 0 \quad . \tag{1}$$

Because equation 1 contains a second-order differential of temperature, any approximation for temperature based upon equation 1 must be second-order differentiable. However, first-order differentiable approximation functions can be utilized if a "weak" formulation of the governing equation is employed. This approach greatly simplifies numerical

approximation of the governing equation. The complete derivation of the following weak formulation (and proof of its uniqueness) is presented by Klett[11]. As Klett[11] explains, the equivalent form of equation 1 over the region Ω is given as

$$-\iint_{\Omega} \begin{bmatrix} \kappa_x & 0 \\ 0 & \kappa_y \end{bmatrix} \vec{\nabla}\hat{T} \cdot \vec{\nabla}\nu \, d\Omega = \iint_{\Omega} \begin{bmatrix} \kappa_x & 0 \\ 0 & \kappa_y \end{bmatrix} \vec{\nabla}\hat{F} \cdot \vec{\nabla}\nu \, d\Omega \quad , \tag{2}$$

where ν is an arbitrary "test" function defined over the region Ω and $\hat{T}$ is a combination of the temperature profile, T, and the interpolated boundary conditions, $\hat{F}(x,y)$ such that:

$$\hat{T}(x,y) = T(x,y) - \hat{F}(x,y) \quad , \quad \forall x,y \in \Omega . \tag{3}$$

Thus, equation 3 is ideal for modeling steady-state heat transfer in an anisotropic multiphase solid. Furthermore, this "weak" formulation is easily solved using the finite element method (FEM).

3. MICROSCOPIC MODEL DEVELOPMENT

3.1 Transverse to the fiber axis.

3.1.1 Mesh Development. The first step in the finite element method is to describe the model geometry and then select the type of mesh which best approximates the model. Figure 2 illustrates the approximate structure of a carbon vapor infiltrated (CVI) or pitch-derived matrix in a carbon-carbon composite. For simplicity, the fibers are arranged in a symmetric pattern. In a real carbon-carbon composite, the fibers would be arranged in a more random pattern.

Because the fibers are cylindrical and the matrix orients in a sheath-like structure, a mesh with triangular elements is more suitable than a mesh with quadrilateral elements, because triangular elements can represent a circle more easily than rectangular elements. If the

temperature profile across the composite is continuous, then piecewise-linear approximation functions should provide sufficient accuracy. Normally, reducing the grid size can compensate for irregularities in the temperature profile. Figure 3(a) illustrates the proposed mesh used to model the thermal properties (transverse to the fiber axis) of a composite reinforced with round fibers.

3.1.2 Material Properties. In a carbon-carbon composite derived from a polymer matrix, there is virtually no structure to the carbon matrix and, thus, the thermal properties of the matrix are locally isotropic (i.e., $\kappa_x \cong \kappa_y$). However, in a composite derived from a pitch matrix, the carbon is arranged in a graphitic structure around the fibers, usually in a sheath-like texture (Figure 1b). The thermal conductivity of graphite, measured parallel to the basal planes, is approximately two orders-of-magnitude greater than that measured perpendicular to the basal planes[12]. Therefore, the matrix elements shown in Figure 3(a) are assigned radially symmetric material properties (about a fiber center), with the thermal conductivity in the θ-direction two orders-of-magnitude greater than that in the r-direction (i.e., $\kappa_\theta \cong 100 \cdot \kappa_r$).

The model is designed to simulate fibers with either random, transverse microstructures (like that observed in T300 PAN-based fibers shown in Figure 1(a)) or radially symmetric microstructures (like that observed in P55 pitch-based fibers shown in Figure 1(b)). To account for random, transverse microstructures, the fiber elements are assigned isotropic material properties (i.e., $\kappa_x \cong \kappa_y$, or $\kappa_\theta \cong \kappa_r$). However, for a composite with P55 fibers, which are radially anisotropic, this is more difficult. It is generally understood that P55 fibers exhibit a flat-layer texture, which, for simplicity, can be approximated by a radial texture in this model. Therefore, the P55 fiber elements can be assigned radially symmetric anisotropic material properties to simulate radially symmetric, transverse microstructures. In this case, the basal planes of the fiber

are oriented in the radial direction (opposite those of the matrix) and the thermal conductivity in the r-direction is two orders-of-magnitude greater than that in the θ-direction (i.e., $\kappa_r \cong 100 \cdot \kappa_\theta$).

The thermal conductivity of a crack is assumed to be negligible compared to that of the matrix or that of the fiber. Thus, elements with thermal conductivities equal to zero (shown in black) can be included to simulate microcracks.

3.2 Parallel to the fiber axis.

The finite element mesh shown in Figure 3(b) was utilized to model thermal conductivity parallel to the fiber axis of composites made with round fibers. In this orientation, both the matrix and the fiber are modeled with Cartesian (x-y) material properties. The matrix elements are assigned anisotropic material properties, with the thermal conductivity parallel to the fiber axis two orders-of-magnitude greater than the thermal conductivity perpendicular to the fiber axis (i.e., $\kappa_z \cong 100 \cdot \kappa_y$). Since the basal planes in the fibers (both PAN-based and pitch-based) are oriented primarily in the direction parallel to the fiber axis, the fiber elements are modeled in a similar manner (i.e., $\kappa_z \cong 100 \cdot \kappa_y$). Again, microcracks and voids (elements with zero thermal conductivity) can be readily distributed throughout the matrix, simulating a porous structure.

3.3 Solution Technique

After the meshes have been generated, the boundary conditions are applied to the mesh, depending on the specific problem. The objective of this research is to estimate the thermal conductivity of the carbon-carbon composites produced in the current study. Thus, by simulating one-dimensional heat transfer, the average thermal conductivity in the x-direction can be predicted for any given structure of carbon-carbon composites. This involves applying a

temperature gradient, $\Delta T/\Delta x$, across the composite section in the x-direction (Dirichlet boundary conditions). To simulate one-dimensional heat flow, the microscopic section is assumed to be insulated along its boundaries at y = 0 and y = B. This is easily accomplished by selecting an interpolating function, $\hat{F}$, that fits this Neuman boundary conditions (Figures 3(a) and 3(b)).

Next, the finite element method is used to solve equation 2 over the region. Then, the temperature profile across the composite is calculated using the post processor. From this profile, the overall heat flux in the x-direction, Q_x, is calculated by integrating the temperature gradient across one side. Finally, the average thermal conductivity in the x-direction, κ_x, is calculated using Fourier's Law as follows:

$$\kappa_x = \frac{Q_x \Delta x}{\Delta T} \quad . \tag{4}$$

Unfortunately, this is the average thermal conductivity for only a composite without microcracks. Real composites will have many different distributions of cracks around the fibers. Therefore, the next step is to calculate the average thermal conductivity in the x-direction for many different distributions of cracks. Microcracks can appear in the matrix or at the fiber/matrix interface, illustrated in Figure 4, depending on the processing. If the cracks are randomly distributed throughout the microscopic section and the thermal conductivity of each configuration determined, then the average thermal conductivity on the microscopic level of a composite with a given volume fraction of microcracks can be estimated. Since the reinforcing fibers are round, the same approach can be utilized to estimate either κ_x or κ_y. By performing this operation repeatedly, with random distributions of cracks, a database of material properties for a microscopic section is generated, which will be used in the overall large-scale model.

4. MACROSCOPIC MODEL DEVELOPMENT

Unfortunately, the above approach only simulates the thermal conductivity of a carbon-carbon on a microscopic level. In an actual composite, many cracks and voids are much larger than these microscopic regions. Therefore, the above approach must be extended to model heat transfer through a typical carbon-carbon composite (illustrated in Figure 5), which is many times larger than the microscopic regions previously described. In this large composite model, the material properties for each rectangular element (broken into two triangular elements for the Finite Element Model) are randomly selected from the database of thermal conductivities for the microscopic sections previously developed. Then, macroscopic pores are distributed throughout the large composite. As with the microscopic sections, a temperature gradient is applied across the composite to determine the thermal profile. Next, the finite element method is utilized to solve equation 2 over the macroscopic composite. The heat flux and the average thermal conductivity is then calculated as before. This process is repeated many hundreds of times to determine an estimated average thermal conductivity of a large composite with a given volume fraction of porosity. Figure 6 is a flow diagram illustrating the path used to predict the thermal properties of an overall composite, utilizing the databases developed on the microscopic level.

5. COMPUTER SOLUTION

A commercial package capable of using both radial symmetric and Cartesian coordinate systems simultaneously and capable of repetitive random distributions of pores or cracks could not be found. Therefore a finite element code was written in FORTRAN to perform the above described model. A preprocessor allowed input of the desired material properties and geometry of the microscopic model. The processor defined the model geometry, mesh

generation, boundary conditions and material properties of each element. Then it utilized the Finite Element Method and equation 2 to develop a system of equations to solve the problem. An iteration scheme was used to solve the system of equations and thereby calculate the temperature at each node in the model. Finally, a post processor integrated the flux across one boundary to calculate the overall flux, Q_x and then calculate the thermal conductivity of the microscopic section. The FORTRAN code then repeated this simulation with a random distribution of microcracks 500 times.

A second code was written to simulate the overall composite. The preprocessor input the model geometry, grid size, etc. Then it randomly selected the material properties for each element from the databases developed from the microscopic models. Next, it randomly distributed porosity throughout the sample. The processor and post processor employed the same techniques to calculate the overall flux, Q_x and then calculate the thermal conductivity of the overall composite. The code then repeated this process over 500 times to determine an average thermal conductivity and a range of possible thermal conductivities for different porosity distributions.

6. MODEL PARAMETERS

6.1 *Microscopic Model*

6.1.1. *Transverse to the fiber axis.* It was found that the model solution changed insignificantly under grid refinement once the size of the largest element in the triangulation was less than 0.1 times the fiber diameter. Therefore, in all subsequent modeling trials transverse to the fiber axis, the largest element size was set at 0.1 times the fiber diameter.

The thermal conductivity of a microscopic section as a function of the relative residue in the iteration asymptotically approached a constant value at or below a residue of $1x10^{-6}$. Therefore, this residue was used in all simulations of thermal conductivity transverse to the fiber axis.

The specific fiber arrangement was the final undetermined parameter needed to model the thermal conductivity transverse to the fiber axis. As described earlier, a symmetric arrangement of two fibers by two fibers was assumed for this study. Typical models only study a unit cell around a fiber. However, in our case pores and cracks can range larger than one unit cell and, thus, the exact number of fibers contained in the microscopic section (both the x- and y-directions) could conceivably affect the numerical solution. Therefore, the influence of the number of simulated fibers, in both the x- and y-directions, on the estimated thermal conductivity in the x-direction was evaluated. These results indicated that a symmetric arrangement of two fibers by two fibers was sufficient to achieve accurate results.

In summary, the parameters chosen to model the thermal conductivity transverse to the fiber axis were as follows: a geometry of two fibers by two fibers, an element size of 0.1 times the fiber diameter, and a residue of $1x10^{-6}$. The final mesh for this model is shown in Figure 9.

6.1.2. *Parallel to the fiber axis.* In a similar manner as just described, it was found that an element size of no greater than 0.16 times the fiber diameter was appropriate for discretization of the region parallel to the fibers.

In this case it was found that an iteration residue of $1x10^{-5}$ was sufficient to minimize irregularities of the solution which might occur because of the pores and cracks.

Unlike with the section transverse to the fiber axis, the number of nodes in the z-direction in this geometry can be variable. Therefore, a similar study as before was performed to determine that 20 nodes in the z-direction was necessary to minimize potential solution irregularities caused by porosity.

Based on these analyses, the final mesh (Figure 10) for modeling the thermal conductivity, parallel to the fiber axis, used the following parameters: 20 nodes in the z-direction, a element size of 0.16 times the fiber diameter, and an residue of $1x10^{-5}$.

6.2 Macroscopic Model

Figure 8 is a typical mesh for modeling the thermal conductivity of an overall composite with large voids and cracks. This will work for modeling heat transfer either parallel to the fiber axis or transverse to the fiber axis, depending only on the database used to select the random distribution of element material properties. Only two parameters are important for the overall macroscopic model: the number of microscopic cells in each direction and the iteration residue. For simplicity, a square grid, with the same number of cells in the x-direction as in the y-direction, was chosen. The overall model was used to determine the number of microscopic cells needed to accurately calculate the thermal conductivity of a large composite. The material properties of each square element were randomly selected from a database of microscopic

thermal conductivities (developed from the previous models). Then, the overall thermal conductivity was calculated using the finite element method described earlier. This calculation was performed over 500 times to determine an average thermal conductivity on the macroscopic level. These results indicate that a minimum of 20 cells in each direction was sufficient in order that the calculated thermal conductivity converged to an asymptotic value.

The next step was to determine the iteration residue needed for this large composite model to asymptotically converge to a solution. For a mesh with 20 cells in each direction, the material properties of each square element were randomly selected, as before. Then, the thermal conductivity of this specific arrangement was calculated for different iteration residues. The results indicate that a residue of $1x10^{-5}$ should yield a satisfactory solution.

6.3 *Composite Variables*

Once the model parameters were determined, the specific material variables (such as fiber fraction, fiber structure, matrix structure, fiber/matrix interface and void fraction) were input into the finite element program. Based on this input, the model then predicted the average thermal conductivity of a particular carbon-carbon composites. To test the model, two composite types made by Klett[13] were used as baseline composites. These composites were made by a towpregging process whereby a Mitsubishi AR mesophase pitch (designated AR-120) was used as the matrix around T300 and P55 carbon fibers. The thermal diffusivity of these composites was measured at room temperature on a Xenon Pulse Flash measurement device at Oak Ridge National Laboratory. The thermal conductivity then was calculated from material properties. The previously mentioned variables described of each specific composite type was determined by optical image analysis and are listed in Table I described below.

6.3.1 *Fiber/Matrix Interface*. The T300/AR-120 composites fabricated by Klett[13] exhibited good bonding between the fiber and the matrix. Conversely, the composites containing pitch-based carbon fibers, P55/AR-120, developed a poor fiber/matrix interface[13]. The model accounted for the poor fiber/matrix interface by placing the cracks at the fiber surface, rather than in the matrix phase. On the other hand, the model simulated the good fiber/matrix interface by placing cracks in the matrix phase, rather than at the fiber surface. Figure 4 illustrates the type of mesh used to simulate a poor fiber/matrix interface and the type of mesh used to model a well-developed fiber/matrix interface.

6.3.2 *Fiber Properties*. As one might expect, the most critical material variables in the model proved to be the thermal conductivities of the fiber and the matrix phases. For the T300 fiber, the transverse texture is essentially random, and therefore, the transverse thermal conductivity was assumed to be isotropic. As a first approximation, the transverse thermal conductivity was assigned a value which was two orders-of-magnitude less than the thermal conductivity parallel to the fiber axis. This approximation is reasonable because other lattice dependent properties of graphite, such as elastic modulus, exhibit a similar trend. (The theoretical modulus in the direction of the basal planes is 1060 GPa, and the theoretical modulus in the transverse direction is 36.5 GPa.[14,15]) The estimated thermal properties of the T300 fibers employed in the model are presented in Table II.

For the P55 pitch-based fibers, the basal planes within the fiber are oriented in the direction of the fiber axis and “primarily” perpendicular to the fiber surface. Thus, the thermal conductivity parallel to the basal planes (or perpendicular to the fiber surface) was assigned a

value equal to the axial thermal conductivity. As before, the thermal conductivity in the direction perpendicular to the basal planes, or the hoop (θ) direction, was assumed to be 0.01 times the thermal conductivity parallel to the basal planes. The exact fiber thermal properties used in the model are presented in Table III.

6.3.3 *Matrix Properties.* Unfortunately, the thermal properties of the matrix are not directly measurable. Therefore, the overall thermal conductivity of the composite is measured and then the matrix properties are typically back calculated using a "rule of mixtures," thus "training" the model with experimental data. Three experimental T300/AR-120 composites were randomly selected from each heat treatment group described in section 6.3 (1100°C and 2400°C) to serve as control samples. A "rule of mixtures" model was used to estimate the thermal conductivity of the matrix in the direction parallel to the fibers (aligned with the basal planes) for each of the control samples. Using this approach, the thermal conductivities of the matrix (parallel to the fibers) in the composites heat treated to 1100°C and 2400°C were estimated to be 6.2 W/m·K and 257 W/m·K, respectively[11]. Again, the thermal conductivity perpendicular to the basal planes of the matrix was assumed to be 0.01 times that parallel to the basal planes, at both heat treatment temperatures.

Because the matrix structure parallel to the fibers is highly linear, this simple "rule of mixtures" model should provide a reasonable prediction of the conductivity of the matrix in the fiber direction. However, predicting the conductivity in the direction transverse to the fiber axis is less straight forward, because the matrix folds and kinks around the fibers during carbonization (heat treatment to 1100°C). As with the thermal conductivity parallel to the fiber axis, the thermal conductivity in the hoop direction around the fiber (θ-direction) is directly related to the crystal structure in this direction. X-ray studies by Klett[13] showed that the crystal structure of the

matrix was not significantly developed at 1100°C. Therefore, as a first approximation, the crystal length in the θ-direction was estimated to be equal to the crystal length in the direction parallel to the fibers. In other words, at 1100°C $L_{a,\theta} = L_{a,z}$. Hence, the thermal conductivity in the θ-direction around the fibers was estimated to be equal to the thermal conductivity in the direction parallel to the fibers, or $\kappa_\theta = \kappa_z$ at 1100°C.

However, this is not expected to be the case at higher heat treatment temperatures. As the matrix is graphitized, the crystalline structure grows parallel to the fibers and the folding around the fibers becomes more distinct (see Figure 7). Since, the thermal conductivity of the graphite crystal is linearly dependent on the crystal length, one would expect that, if the crystal length in the θ–direction, $L_{a,\theta}$, is less than that in the direction parallel to the fiber axis, $L_{a,z}$, the thermal conductivity of the matrix should follow a similar trend. Unfortunately, it is virtually impossible to determine the crystal length of the basal planes in the θ–direction, and thus, the crystal length of the matrix (heat treated to 1100°C) in this direction was simply assumed to be ~1/4 of that parallel to the fiber axis, or $L_{a,\theta} \approx 1/4\ L_{a,z}$. Hence, $\kappa_\theta \approx 1/4\ \kappa_z$ at 2400°C. The estimated thermal properties of the matrix, at both heat treatment temperatures, are presented in Table IV.

7. MODEL RESULTS

7.1 *T300-based composites*.

Using these estimates for the fiber and matrix thermal properties, the thermal conductivities of the remaining T300/AR-120 composites (at each heat treatment temperature) were predicted by the finite element model. First, the databases produced by modeling heat transfer through the microscopic sections were utilized as input to the overall composite model. Based on this input, the overall composite model estimated the thermal conductivity of the large

composites with different fiber fractions and void fractions. The results are presented in Tables V - VII, along with the measured thermal conductivities of the T300/AR-120 samples.

It is apparent that the model accurately predicts the thermal conductivity, both parallel and transverse to the fiber axis, for the T300/AR-120 composites heat treated to 1100°C and 2400°C. In fact, the average predicted thermal conductivity is within the 95% confidence interval of the average measured thermal conductivity. While the difference between the measured and predicted values is greater for the transverse model, the model still appears to be predict thermal conductivity reasonably well.

For the two cases where heat transfer is parallel to the fiber axis, most of the predicted values fall within 10% of the measured values, and all of the predicted values are within 20% of the measured values. Since the composite microstructure, fiber distribution and crack distribution in the actual composites can vary significantly, this degree of accuracy is quite surprising.

However, when heat transfer is transverse to the fiber axis, some model predictions deviate by more than 20% from the measured values. This increased scatter is not surprising since the heat flow transverse to the fibers is more likely to be interrupted by cracks and irregularities in the composite, common imperfections in carbon-carbon. As shown in Table VII, the largest discrepancies are when the porosity of the composites are very low. If large regions of matrix running from one side to the other are present, (which can be common in pitch derived carbon matrices, then the measured transverse thermal conductivity will be higher than that predicted by the model. Conversely, if the specimen contains large regions of pores which disrupt heat flow, then the predicted thermal conductivity will be greater than the measured

value. Obviously, the model is not as sensitive to porosity and matrix structures compared to a real composite.

In summary, one would expect more scatter between the measured and the predicted thermal conductivities of the transverse samples. The model could be refined to account for globally large regions of matrix and/or voids to simulate more closely a pitch-derived composite. Nevertheless, the model appears to provide an accurate estimate for the average transverse thermal conductivity of T300/AR mesophase pitch carbon-carbon composites.

7.2 P55-based composites.

To demonstrate the model's versatility, the technique then was extended to predict the thermal properties of different types of composites (P55/AR-120) produced by Klett[13]. First, the databases of thermal conductivities for the microscopic sections (P55 carbon-fibers) were developed using the matrix material properties determined for the T300/AR-120 composites. These databases then were utilized as input to the overall computer model. The results of the large composite models are presented in Table VIII, along with the measured thermal conductivities for the P55/AR-120 carbon-carbon composites produced by Klett[13]. It should be noted that the model was trained with data from a different family of composite (one containing T300 fibers) than the one being modeled.

As shown in Table VIII, the model was able to accurately predict the thermal behavior of the P55/AR-120 composites which were heat treated to 1100°C. From this, one can assume that the matrix properties in the T300/AR-120 and the P55/AR-120 composites were similar. However, the model's accuracy decreased as the final heat treatment temperature increased to 2400°C. For instance, while the model accurately predicts the properties of the T300/AR-120

composites heat treated to 2400°C, the estimated thermal conductivity of the P55/AR-120 composites heat treated to 2400°C was nearly 23% greater than the average measured for the four composite samples. It appears that the matrix will develop a different level of thermal conductivity depending on the type of reinforcing fiber (T300, P55) in the composite. This effect has been confirmed by numerous studies[16, 17].

From the above results, it is clear that the model was able to account for the differences in the fiber morphology, and the interfacial bonding, varying porosity and fiber fractions in the composites reinforced with round fibers. Most other models do not account for either the fiber morphology or the fiber/matrix interface[3 - 7].

8. GENERAL DISCUSSION

From this work it is clear that the thermal conductivity of carbon-carbon composites can be modeled and, therefore, predicted using the Finite Element Method. To predict the thermal conductivity of carbon-carbon, the fiber fraction, void fraction, crack pattern, fiber/matrix interface, microscopic voids, macroscopic voids, orientation of the matrix, and the thermal properties of the fibers and the matrix must be provided. However, when these properties are not known precisely, the model can still yield important fundamental knowledge concerning the thermal transport behavior of carbon-carbon composites. In the following sections, the model is used to determine how fiber texture, fiber/matrix interface, and relative fiber thermal conductivity can affect the thermal conductivity of carbon-carbon composites. These test cases illustrate the model's ability to predict potential trends and effects.

8.1 *Effects of Fiber Texture on Overall Thermal Conductivity*

Assume that two types of high thermal conductivity fibers, with the same axial thermal conductivity but different transverse morphology, are available for a manufacturing process. The designer needs to know which will yield the optimum composite thermal conductivity. For instance, will a radial morphology or an onion skin morphology improve the transverse thermal conductivity of the composite? The influence of these two different fiber morphologies on transverse thermal conductivity is shown in Figure 8. In this case, the thermal conductivity of both fibers was assumed to be 1000 W/m·K parallel to the fiber axis. Therefore, for the fiber with a radial texture (P55 Fibers), the thermal conductivity in the r-direction was assumed to be 1000 W/m·K, and the thermal conductivity in the θ–direction was set at 10 W/m·K. On the other hand, for the fiber with an onion skin texture (Vapor Grown Fibers), the thermal conductivity in the r-direction was assumed to be 10 W/m·K, and the thermal conductivity in the θ–direction was set at 1000 W/m·K. The mesh shown in Figure 3(a) was used in these simulations. The matrix was assumed to possess a sheath-like structure, and the influence of the fiber morphology was studied for various matrix thermal conductivities. To isolate the effect of the fiber morphology, voids were not included in the matrix region. As seen in Figure 8 the model predicts that the transverse thermal conductivity of a carbon-carbon composite reinforced with radial fibers would be approximately 20% greater than that of a carbon-carbon composite reinforced with onion skin fibers, even though the thermal conductivity in the direction parallel to the fibers is identical. Therefore, when transverse thermal conductivity is important, fibers with radial textures should out-perform those with onion skin textures (if the fibers have similar axial thermal conductivities).

Figure 9 shows the temperature profiles across a hypothetical composite reinforced by a fiber with an onion skin texture and a composite reinforced by a fiber with a radial texture

(Vapor Grown Carbon Fiber). This example illustrates the effects of different fiber morphologies on the temperature gradients through the composite. Figure 10 shows the fluxes through the two micro-composites. As seen in Figure 10, the structure of the radial fiber permits heat to be transferred to and from the center of the fiber, whereas heat tends to flow around the circumference of the onion skin fiber. This difference in the effective length of heat transfer is the underlying reason why heat is more readily transmitted through the radial fiber composite, and explains its higher transverse thermal conductivity.

8.2 *Effect of Fiber/Matrix Bonding on Overall Thermal Conductivity*

Another design consideration in the manufacture of composites is the location of the microcracks. Is it better for them to be located at the fiber/matrix interface or in the matrix phase? To study this phenomenon, the model was used to simulate two carbon-carbon composites with similar fiber fractions, anisotropic matrix, porosities and material properties, but with different interfaces. The results, presented in Figure 11, indicate that a composite with a poor fiber/matrix interface will exhibit a higher thermal conductivity, both transverse and parallel to the fiber axis, than a composite with a strong fiber/matrix interface. Presumably, this is because the poor interface implies that fewer cracks are present in the matrix at the same porosity level, allowing for better heat flow through the composite. As the composite is densified and the microcracks are eliminated, these differences will become minimal. However, since it is virtually impossible to eliminate all cracks, it is important to appreciate this peculiar role of the fiber/matrix interface, if one hopes to optimize the thermal conductivity of this class of composites.

8.3 *Effect of Fiber Transverse Conductivity on Overall Thermal Conductivity*

Finally, the model was used to study the effect of the transverse fiber conductivity on the overall transverse conductivity of the composite. Figure 12 is a graph of the relative bulk thermal conductivity versus the relative transverse fiber conductivity (both relative to the transverse matrix conductivity) for composites with an isotropic matrix and an anisotropic matrix. The specific material variables are presented in the figure. These results indicate that transverse thermal conductivity of a composite reaches a limiting value when the transverse conductivity of the reinforcing fiber is two orders-of-magnitude greater than that of the matrix. The transverse thermal conductivity of the composite is limited to approximately 3 times that of an isotropic matrix and only 1.3 times that of an anisotropic matrix, with a sheath structure. For a composite with an isotropic matrix, this result is similar to that reported by Grove[6]. This effect is important for composites in which transverse thermal conductivity is critical, such as circuit board substrates and first wall material for fusion reactors. In these applications, the principal objective is to transfer the heat into the composite (in the transverse direction) and then wick it away from the source with the fibers. Typically, design of these composites focuses on the selection of the fibers and the orientation of the reinforcement. Clearly, this analysis shows that the selection of the matrix may be equally important.

For instance, applications such as satellite substrates utilize unidirectional carbon-carbon composites made with high thermal conductivity carbon fibers (i.e. K1100). The intent of using the K1100 fibers is to improve the effectiveness of removing heat from electrical components. However, we have shown that with a unidirectional composite, the thermal conductivity in the transverse direction can only be roughly 3 times greater than the transverse thermal conductivity

of an isotropic matrix. In other words, the fibers offer very little advantage in the transverse direction. This is a extremely important fact since the heat must first be conducted in transverse direction before it is conducted away from the heat source. Therefore, the designers should put as much emphasis on utilizing a high conductivity matrix as they do to utilize high conductivity fibers. In fact, since some fibers can cost as high as $1000 dollars per pound, switching from a phenolic derived matrix (low conductivity) to a pitch derived matrix (high conductivity) may be a less expensive path to the same result as switching to a high conductivity fiber.

9. CONCLUSIONS

The current research focused on developing a comprehensive model which can account for the many different variables that influence the thermal conductivity of carbon-carbon. We have shown that the Finite Element Method can be used to simulate the anisotropic, three phase structure of carbon-carbon composites. By modeling the fiber morphology, matrix morphology, fiber matrix interface, void fraction and the random distribution of cracks, pores, and fibers, the thermal behavior of the composites, both parallel and transverse to the fibers, can be predicted. The model also was shown to be reasonably accurate for a wide range of fiber and void fractions. Unfortunately, this type of model cannot predict material properties for use in structural and thermal analysis which are based on continuum (closed form) solutions. Therefore, if one requires the coupling of thermal analysis with mechanical and structural analysis, this type of modeling program will have to be included in any package that will be used. In fact, the mechanical and structural analysis of this type of carbon-carbon should probably be based on a similar micro-mechanical to macro-mechanical modeling.

Finally, although the model must first be “trained” in order to predict the actual thermal conductivity of specific types of composites, the model does not need to be “trained” in order to isolate the effects of specific material characteristics, such as fiber texture or fiber volume fraction, on the composite thermal conductivity. Basically, the designer can determine if the fiber/matrix interface plays a more dominant role that fiber volume fraction in the transverse thermal conductivity. By understanding concepts such as these, attention can be placed on the most significant aspect of the carbon-carbon thermal properties, which should lead to the development of tailored composites specifically designed to fit different needs and reduce costs.

References

1. Pilling, M.W., B. Yates, M.A. Black, and P. Tattersall, *J. Mater. Sci.* **14** (1979).

2. Dawson, D. M., A. Briggs, *J. Mater. Sci.*, **16** (1981), pp. 3356-3356.

3. Whittaker , A. J. and R. Taylor, "Thermal Properties of Carbon-Carbon fibre Composites. I. Thermal Transport Measurement," *Proc. R. Soc. Lond.*, **430** (1991) p. 167.

4. Whittaker , A. J. and R. Taylor, "Thermal Properties of Carbon-Carbon fibre Composites. II. Microstructural Characterization,"*Proc. R. Soc. Lond.*, **430** (1991) p.183.

5. Whittaker , A. J. and R. Taylor, "Thermal Properties of Carbon-Carbon fibre Composites. III. Mathematical Modelling,"*Proc. R. Soc. Lond.*, **430** (1991) p. 199.

6. Grove, S. M., *Comp. Sci. and Tech.*, **38**:199 (1990)

7. J. T. Mottram and R. Taylor, *Comp. Sci. Tech.* **29** (1987) pp. 211-232.

8. Benveniste, T. Chen and G. J. Dvorak, *J. Appl. Phys.* **67** (1990) pp. 2878-2884.

9. V. V. Jikov, S. M. Kozlov, and O. A. Oleinik, "Homoginization of Differential Operators and Integral Functionals," *Springer-Verlag*, (1994).

10. Ervin, V. J., J. W. Klett, and C. M. Mundt, "Estimation of the Thermal Conductivity of Composites," *J. Mat. Sci.***,** in press.

11. Klett , J. W., "Heat Transfer in Carbon-carbon Composite Materials," Ph. D. Dissertation, Clemson University, Clemson, SC (1994).

12. Kelly, B. T., in Physics and Chemistry of Carbon, **5** (1969) p. 119.

13. Klett, J. W. and D. D. Edie, "Flexible Towpreg for the Fabrication of High Thermal Conductivity Carbon-Carbon Composites," *Carbon* , **33**(10) (1995) pp. 1485-1503.

14. Fitzer, E., "The Future of Carbon-Carbon Composites," *Carbon*, **25**(2) (1987) p. 163-190.

15. Edie, D. D., "Pitch and Mesophase Fibers," in Carbon Fibers, Filaments and Composites, Figueiredo (editor), Kluwer Academic Publishers, Boston, (1990) pp. 43-72.

16. Jaklitch, D. J., and J. W. Walkinshaw, "Off-Axis Thermal Conductivity Measurement of Carbonaceous Material by a Modified Pulse Method," *Extended Abstracts-18th Biennial Conference on Carbon*, (1987) p. 284.

17. Fitzer, E., W. Hüttner, and L. M. Manocha, "Influence of Process Parameters on the Mechanical Properties of Carbon-Carbon Composites with Pitch as Matrix Precursor," *Carbon*, **18** (1980) p. 291.

18. Lavin, J. G., D. R. Boyington, J. Lahijani, B. Nysten, J.-P. Issi, “The Correlation of Thermal Conductivity with Electricial Resistivity in Mesophase Pitch-based Carbon Fibers,” *Carbon*, **31** (1993) p. 1001.

List of Tables

Table I. Average variables determined by optical image analysis of the composite specimens measured for thermal conductivity.

Table II. Thermal properties used to model the T300 fibers.

Table III. Thermal properties used to model the P55 fibers.

Table IV. Thermal properties of the pitch matrix at different heat treatments used in both the models parallel and transverse to the fiber axis.

Table V. Measured and predicted thermal conductivity, parallel to the fibers, of T300/AR-120 composites heat treated to 1100°C.

Table VI. Measured and predicted thermal conductivity, parallel to the fibers, of T300/AR-120 composites heat treated to 2400°C.

Table VII. Measured and predicted thermal conductivity, transverse to the fibers, of T300/AR-120 composites heat treated to 2400°C.

Table VIII. Measured and predicted thermal conductivities for P55/AR-120 carbon-carbon composites.

Table I. Average variables determined by optical image analysis of the composite specimens measured for thermal conductivity.

Composite Designation	Final Heat Treatment Temp. (°C)	Fiber Volume Fraction	Microscopic Void Fraction (Cracks)	Overall Void Fraction	Fiber/ Matrix Interface	Fiber Microstructure
T300/AR-120						
Parallel	1100	37.0%	6%	32.9%	Good	Random
	2400	58.3%	5%	26.1%		
Transverse	2400	55.0%	5%	30.6%	Good	
P55/AR-120						
Parallel	1100	61%	12%	18%	Poor	Radial/Flat-Layer
	2400	60%	12%	19%		
Transverse	1100	61%	12%	18%	Poor	

Table II. Thermal properties used to model the T300 fibers.

Fiber	Final Heat Treatment Temperature [°C]	Thermal Conductivity	
		Fiber Axis Z-direction	Transverse Direction X-Ydirection
	[°C]	[W/m·K]	[W/m·K]
T300	1100	8.5 [a]	0.085
	2400	76 [a]	0.76

[a] Estimated from electrical resistivity data with the Lavin relation[18].

Table III. Thermal properties used to model the P55 fibers.

Fiber	Final Heat Treatment Temperature [°C]	Thermal Conductivity		
		Fiber Axis	Transverse Direction	
			Parallel to Basal Plane	Perpendicular to Basal Plane
	[°C]	[W/m·K]	[W/m·K]	[W/m·K]
P55	1100	113 [a]	113	1.13
	2400	196 [a]	196	1.96

[a] Estimated from electrical resistivity data with the Lavin relation[18].

Table IV. Thermal properties of the pitch matrix at different heat treatments used in both the models parallel and transverse to the fiber axis.

Final Heat Treatment	$\frac{L_{a,\theta}}{L_{a,z}}$	Thermal Conductivity			
		Model Parallel to Fiber Axis		Model Transverse to Fiber Axis	
		Parallel to Basal Plane (Z-direction)	Perpendicular to Basal Plane (Y-direction)	Parallel to Basal Plane (θ-direction)	Perpendicular to Basal Plane (R-direction)
		[W/m·K]	*[W/m·K]*	*[W/m·K]*	*[W/m·K]*
1100	1	6.2[a]	0.06	6.2	0.06
2400	1/4	257[a]	2.57	64.3	0.64

[a] Calculated from experimental data using the "rule of mixtures"

Table V. Measured and predicted thermal conductivity, parallel to the fibers, of T300/AR-120 composites heat treated to 1100°C.

Sample ID	Fiber Volume Fraction	Porosity	Measured Thermal Conductivity	Predicted Thermal Conductivity
	[%]	[%]	κ [W/m·K]	κ [W/m·K]
1A-1	48.5	12.7	5.90	6.14 ± 0.45
1B-1	48.5	12.5	6.10	6.17 ± 0.45
1A-2	34.5	28.2	4.42	5.10 ± 0.69
1B-2	34.5	33.1	4.79	4.72 ± 0.74
1C-2	34.5	34.8	4.86	4.63 ± 0.78
1D-2	34.5	34.8	4.62	4.63 ± 0.78
1E-2	34.5	31.7	4.47	4.81 ± 0.77
1F-2	34.5	29.4	4.59	5.06 ± 0.72
1G-2	34.5	38.3	4.79	4.42 ± 0.79
1H-2	34.5	36.2	4.74	4.57 ± 0.80
1I-2	34.5	33.3	5.26	4.75 ± 0.76
2A-2	34.5	41.2	4.59	4.29 ± 0.71
2B-2	34.5	35.3	4.71	4.67 ± 0.79
2C-2	34.5	37.0	4.98	4.56 ± 0.77
2D-2	34.5	37.8	5.11	4.50 ± 0.75
2E-2	34.5	34.2	4.71	4.68 ± 0.76
2F-2	34.5	38.9	4.42	4.39 ± 0.80
2G-2	34.5	39.1	4.54	4.34 ± 0.79
2H-2	34.5	39.2	5.00	4.37 ± 0.80
2I-2	34.5	41.5	4.52	4.27 ± 0.84
Average	**37.0**	**32.9**	**4.86**	**4.75**
95% Confidence	2.9	3.6	0.21	0.24

± denotes standard deviation for more than 500 simulations

Table VI. Measured and predicted thermal conductivity, parallel to the fibers, of T300/AR-120 composites heat treated to 2400°C.

Sample ID	Fiber Volume Fraction	Porosity	Measured Thermal Conductivity	Predicted Thermal Conductivity
	[%]	[%]	κ [W/m·K]	κ [W/m·K]
2A-1	64.2	10.0	97.1	96.4 ± 5.2
2B-1	62.6	14.7	88.7	91.5 ± 7.1
2C-1	60.5	16.0	91.0	90.9 ± 7.5
3A-2	58.1	25.2	91.8	80.4 ± 9.7
3B-2	58.1	26.5	76.7	79.6 ± 10.4
3C-2	58.1	22.3	79.0	83.9 ± 9.8
3D-2	58.1	24.5	80.3	82.3 ± 10.1
3E-2	58.1	27.2	67.1	79.5 ± 10.5
3F-2	58.1	24.8	87.1	82.2 ± 10.0
3G-2	58.1	23.1	79.6	84.0 ± 9.7
3H-2	58.1	26.5	66.9	80.7 ± 10.2
3I-2	58.1	24.2	79.2	83.7 ± 9.5
5B-2	44.0	39.8	62.0	66.9 ± 12.0
5C-2	44.0	37.1	78.6	70.1 ± 11.6
5D-2	44.0	36.5	78.1	70.4 ± 11.5
5E-2	44.0	36.8	73.0	70.9 ± 11.5
5F-2	44.0	39.6	73.2	66.7 ± 12.0
5G-2	44.0	38.3	67.2	69.2 ± 12.1
6A-2	59.8	25.5	82.2	82.1 ± 10.1
6B-2	59.8	23.7	83.3	84.9 ± 9.1
6C-2	59.8	28.5	77.3	79.0 ± 10.5
6D-2	59.8	24.3	87.8	83.7 ± 9.5
6E-2	59.8	27.7	82.8	79.1 ± 10.6
6F-2	59.8	23.9	84.4	83.2 ± 9.4
6G-2	59.8	22.3	88.5	86.7 ± 8.8
7A-2	51.3	28.7	85.8	78.8 ± 10.6
7B-2	51.3	28.5	83.9	78.9 ± 10.6
7C-2	51.3	27.0	89.7	79.4 ± 10.6
7D-2	51.3	26.8	85.2	79.6 ± 10.5
7E-2	51.3	27.6	85.2	79.1 ± 10.7
7F-2	51.3	26.6	87.0	81.2 ± 9.8
7G-2	51.3	27.0	90.8	79.4 ± 10.6
Average	**54.0**	**28.3**	**80.5**	**80.1**
95% Confidence	2.2	1.9	2.7	2.4

± denotes standard deviation for more than 500 simulations

Table VII. Measured and predicted thermal conductivity, transverse to the fibers, of T300/AR-120 composites heat treated to 2400°C.

Sample ID	Fiber Volume Fraction	Porosity	Measured Thermal Conductivity	Predicted Thermal Conductivity
	[%]	[%]	κ [W/m·K]	κ [W/m·K]
3A-1	54.3	7.3	10.2	8.91 ± 0.48
3B-1	57.3	8.6	16.1	8.65 ± 0.50
3C-1	60.6	11.0	16.1	8.04 ± 0.56
9A-2	40.7	41.9	3.84	5.67 ± 1.20
9B-2	40.7	42.9	4.79	5.56 ± 1.21
9C-2	40.7	44.5	3.32	5.39 ± 1.22
9D-2	40.7	45.6	4.12	5.31 ± 1.22
9E-2	40.7	38.8	9.59	5.94 ± 1.17
9F-2	40.7	44.6	5.96	5.39 ± 1.22
10A-2	60.6	25.0	6.82	7.30 ± 0.84
10B-2	60.6	32.3	5.57	6.59 ± 1.01
10C-2	60.6	25.9	6.38	7.26 ± 0.94
10D-2	60.6	26.3	6.66	7.18 ± 0.98
10E-2	60.6	28.0	6.19	6.92 ± 0.98
11A-2	48.6	26.0	5.24	7.21 ± 0.87
11B-2	48.6	33.0	6.50	6.57 ± 0.99
11C-2	48.6	29.9	6.64	6.72 ± 0.95
11D-2	48.6	31.7	6.44	6.68 ± 0.96
11E-2	48.6	28.9	6.11	6.93 ± 0.94
11F-2	48.6	27.2	7.40	7.09 ± 0.90
11G-2	48.6	29.1	5.86	6.80 ± 0.98
12B-2	58.4	27.0	6.28	7.12 ± 1.18
12D-2	58.4	23.8	7.35	7.43 ± 0.86
12E-2	58.4	29.6	6.78	6.77 ± 1.01
Average	**51.2**	**32.6**	**7.09**	**6.80**
95% Confidence	3.1	4.7	1.33	0.40

± denotes standard deviation for more than 500 simulations

Table VIII. Measured and predicted thermal conductivities for P55/AR-120 carbon-carbon composites.

Composite	Final Heat Treatment	Parallel to the Fiber Axis			Transverse to the Fiber Axis		
		Measured κ	# of Samples	Predicted κ	Measured κ	# of Samples	Predicted κ
P55/ AR-120	1100	70.8 ± 3.7	4	67.5	2.4 ± 0.4	5	2.20
	2400	135.5 ± 4.3	4	165.7	--	--	--

± denotes a 95% confidence interval

List of Figures

Figure 1. Photomicrograph of two different carbon-carbon composites, illustrating the variation in structure commonly observed.

Figure 2. Illustration of sheath-like matrix orientation in composites reinforced with round fibers.

Figure 3(a). Triangular mesh used to model thermal conductivity transverse to the fiber axis of a microscopic composite section.

Figure 3(b). Triangular mesh used to model thermal conductivity parallel to the fiber axis of a microscopic composite section.

Figure 4. Finite element mesh with (a) a poor fiber/matrix interface and (b) a good fiber/matrix interface.

Figure 5. Triangular mesh used to model heat transfer through a large composite.

Figure 6. Flow diagram illustrating method used to model the overall thermal conductivity of a composite.

Figure 7. Folding of crystal structure of the matrix around the fiber at a heat treatment temperature of 2400°C.

Figure 8. Thermal conductivity of a microscopic section with radial and onion skin fibers.

Figure 9. Temperature profile in a composite with (a) a radial fiber and (b) an onion skin fiber.

Figure 10. Map of fluxes in a composite with (a) a radial fiber and (b) an onion skin fiber.

Figure 11. Thermal conductivity of a composite section, transverse to the fibers, with good and poor fiber/matrix interfaces.

Figure 12. Plot of bulk composite transverse thermal conductivity versus transverse fiber conductivity relative to the matrix conductivity.

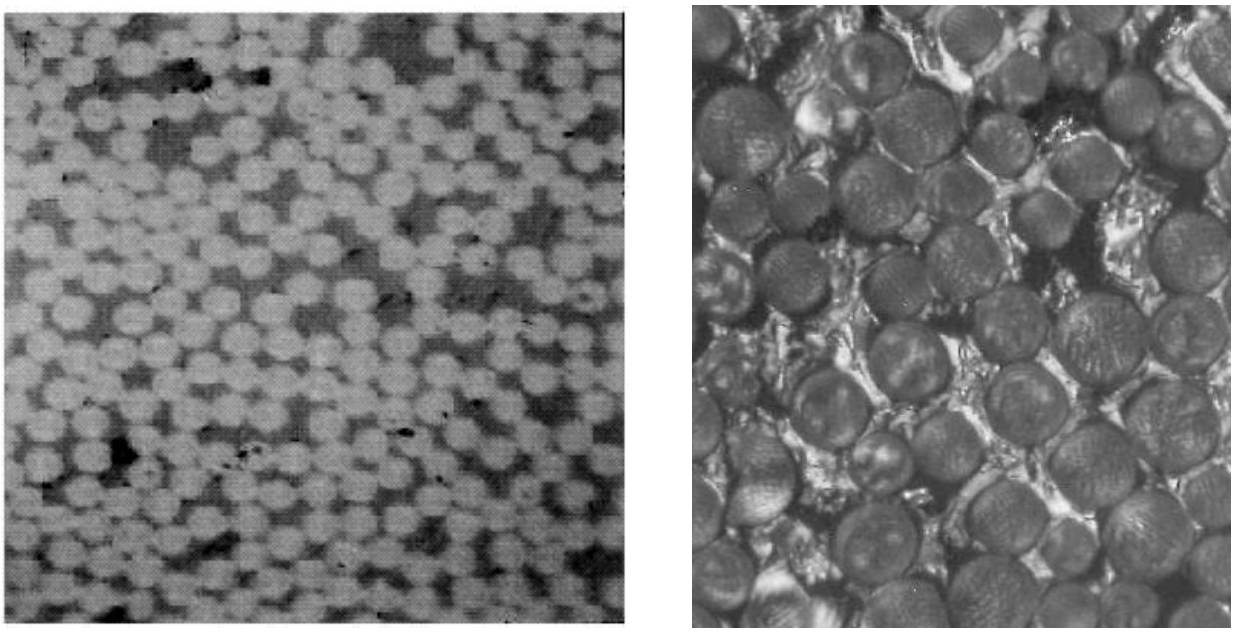

(a) PEEK/AS4 (b) Pitch/P55

Figure 1. Photomicrograph of two different carbon-carbon composites, illustrating the variation in structure commonly observed.

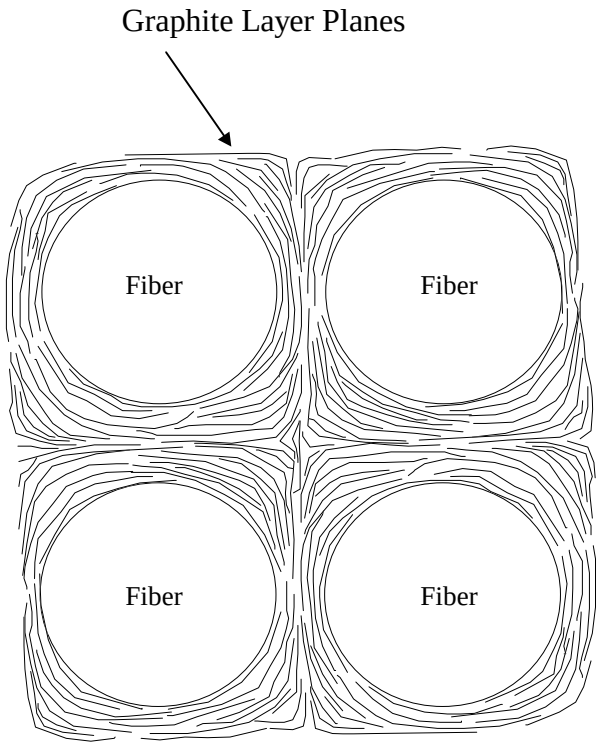

Figure 2. Illustration of sheath-like matrix orientation in composites reinforced with round fibers.

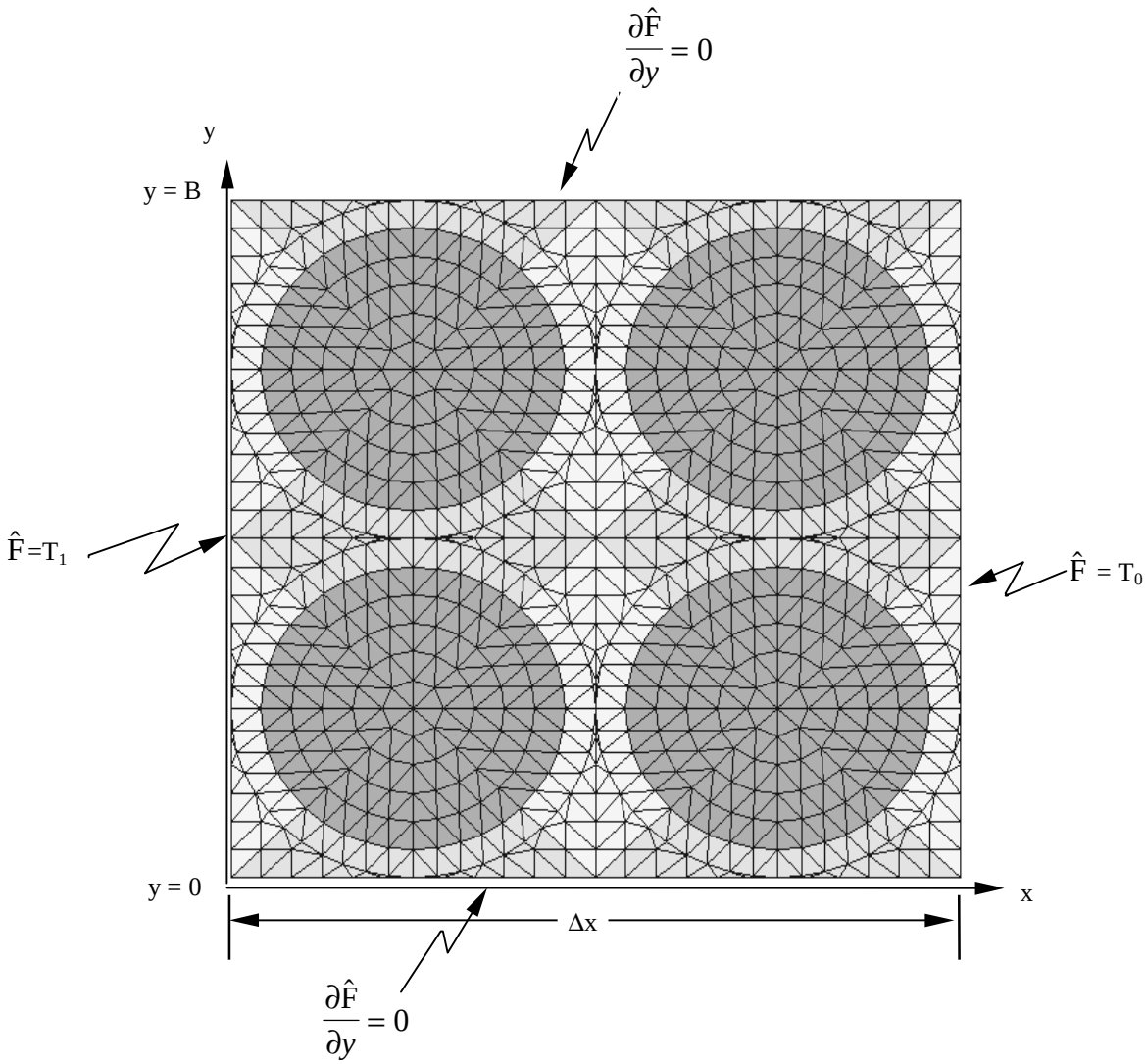

Figure 3(a). Triangular mesh used to model thermal conductivity transverse to the fiber axis of a microscopic composite section.

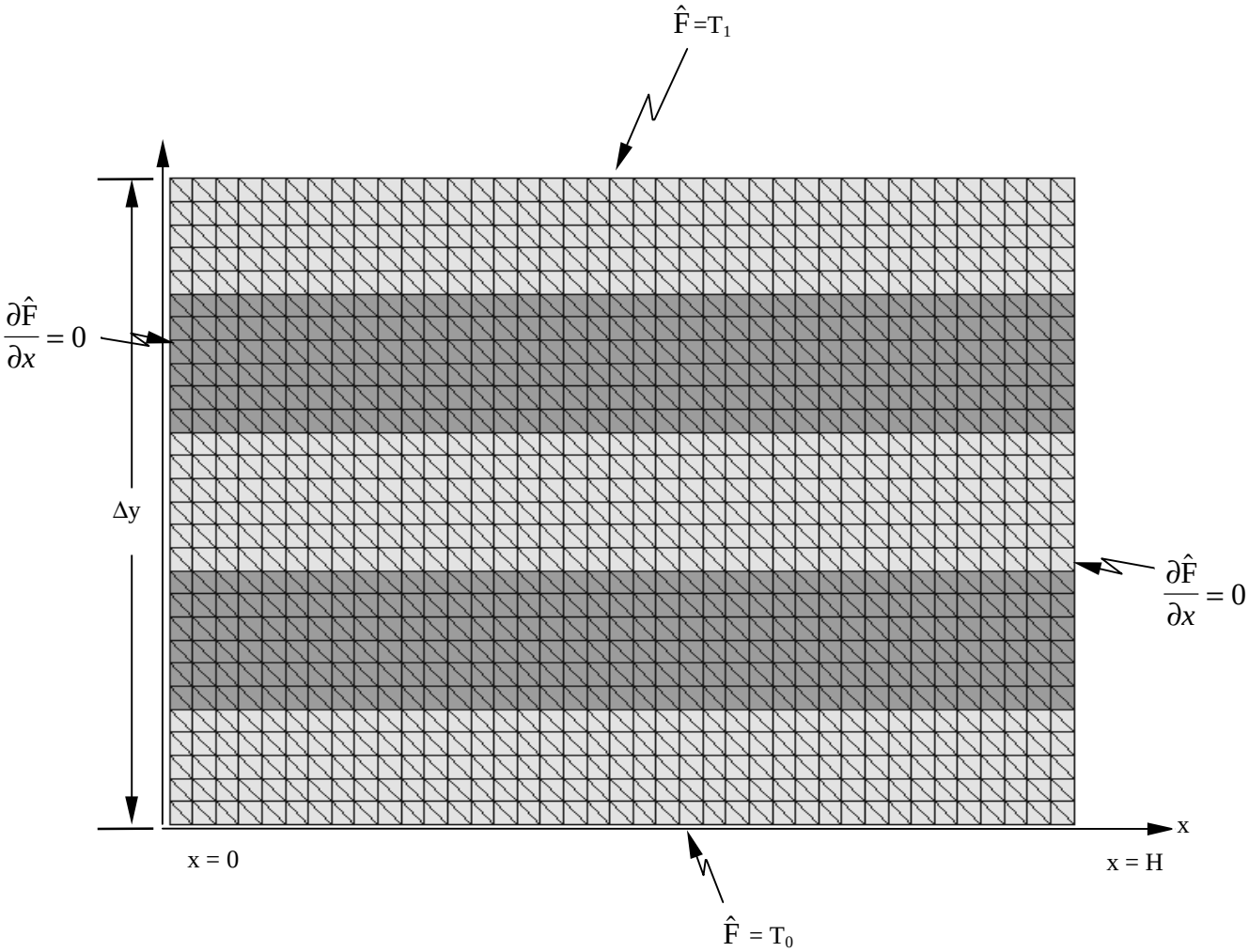

Figure 3(b). Triangular mesh used to model thermal conductivity parallel to the fiber axis of a microscopic composite section.

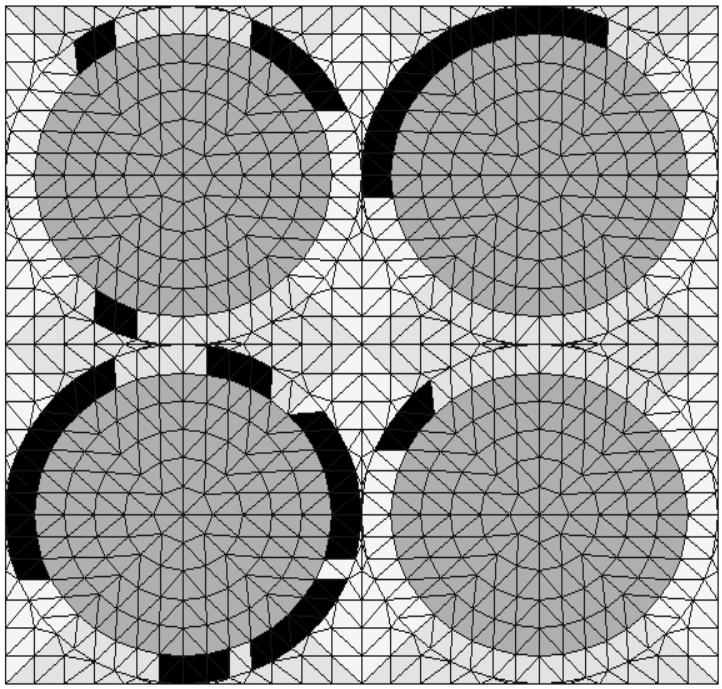

(a)

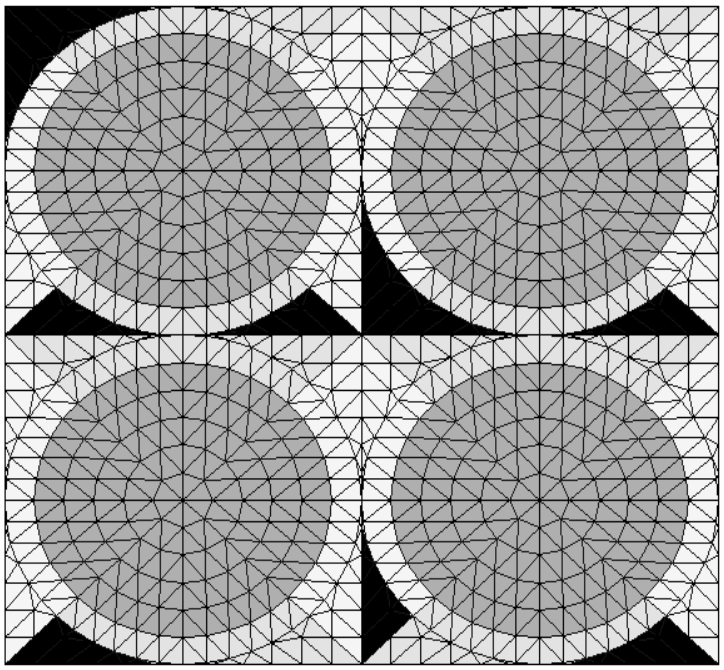

(b)

Figure 4. Finite element mesh with (a) a poor fiber/matrix interface and (b) a good fiber/matrix interface.

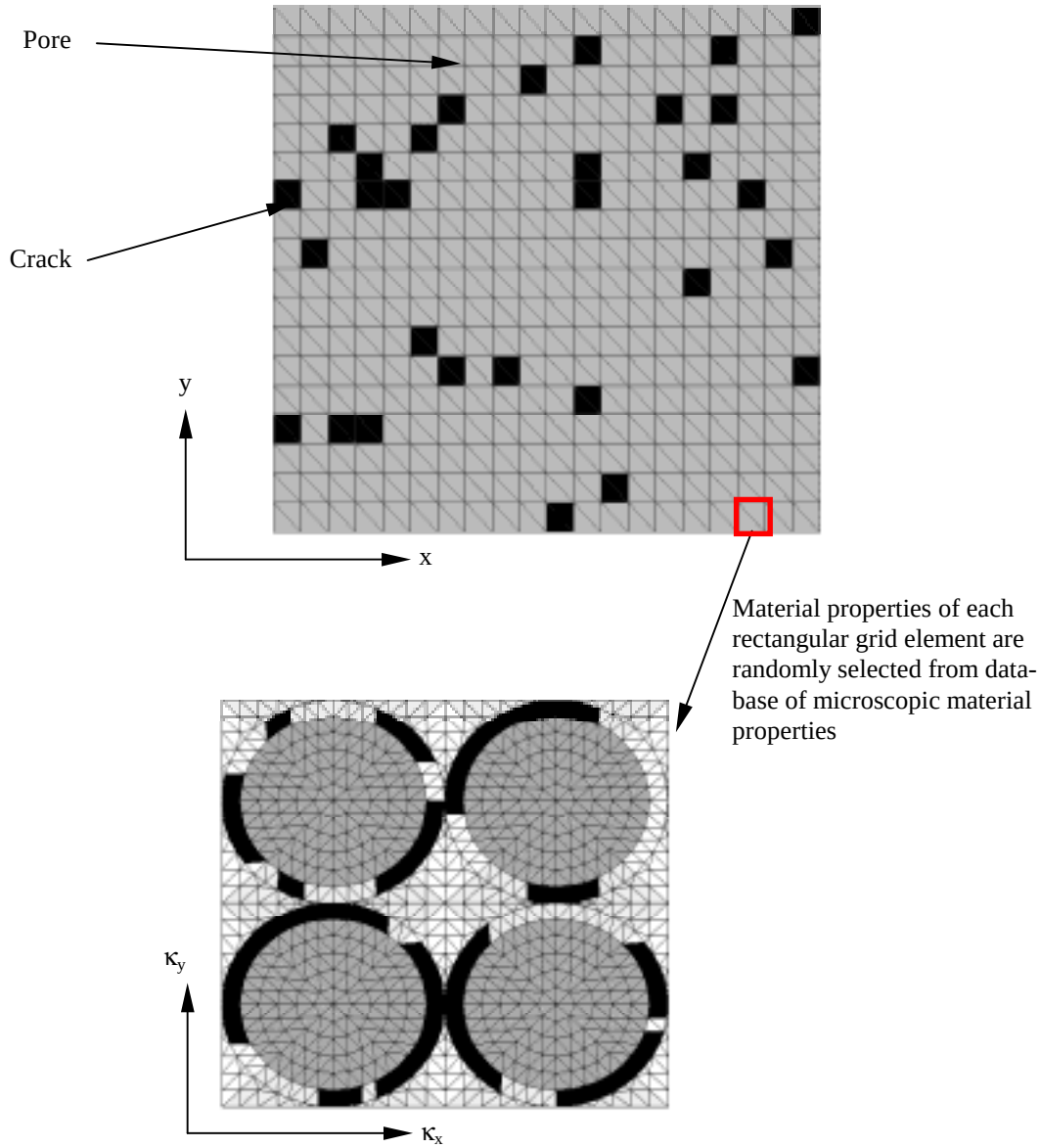

Figure 5. Triangular mesh used to model heat transfer through a large composite.

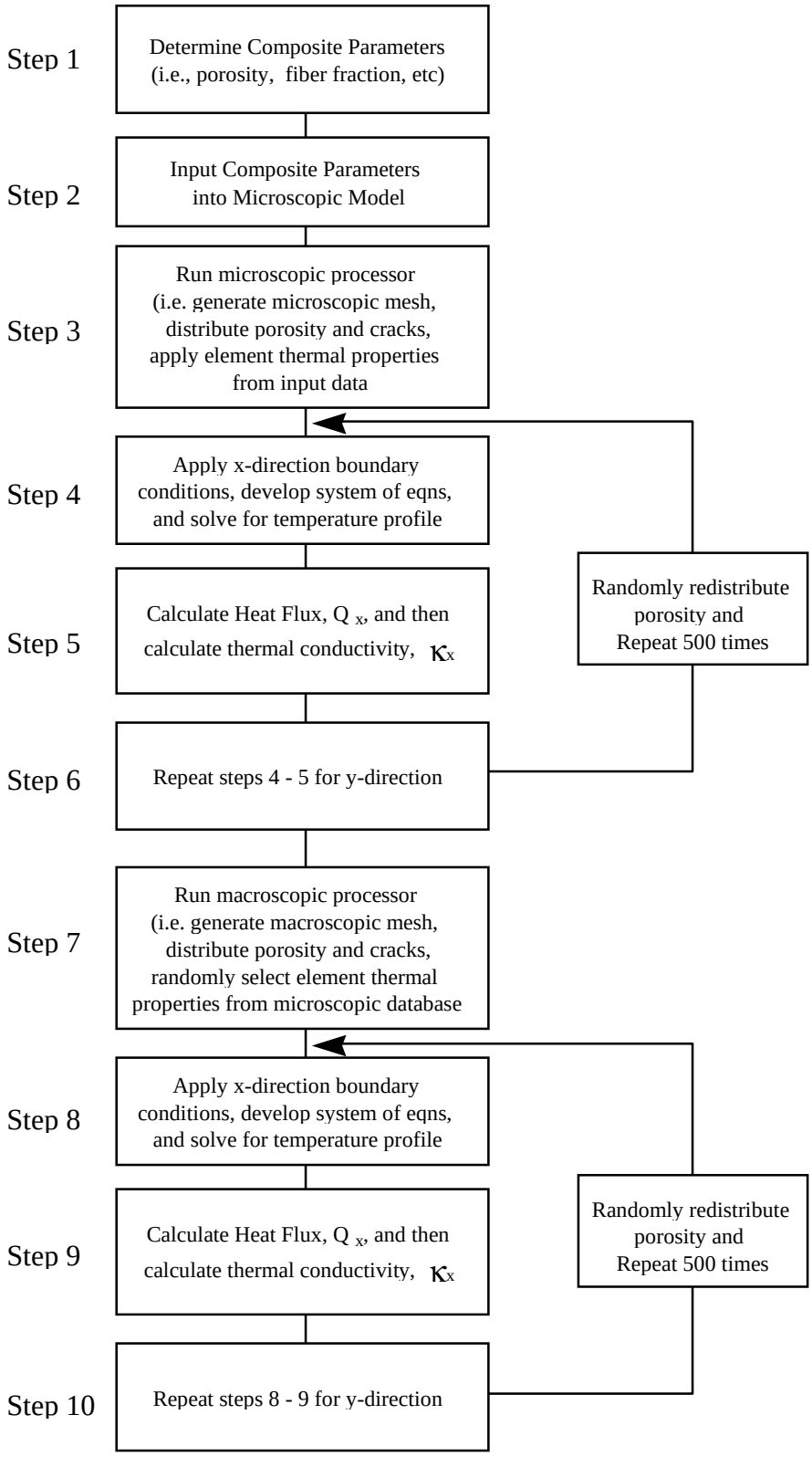

Figure 6. Flow diagram illustrating method used to model the overall thermal conductivity of a composite.

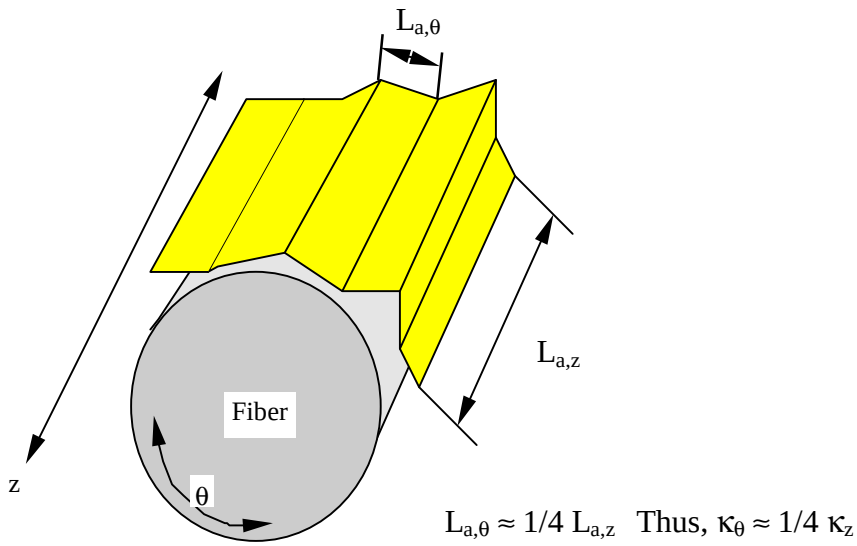

Figure 7. Folding of crystal structure of the matrix around the fiber at a heat treatment temperature of 2400°C (the folding effect has been enhanced for illustrative purposes).

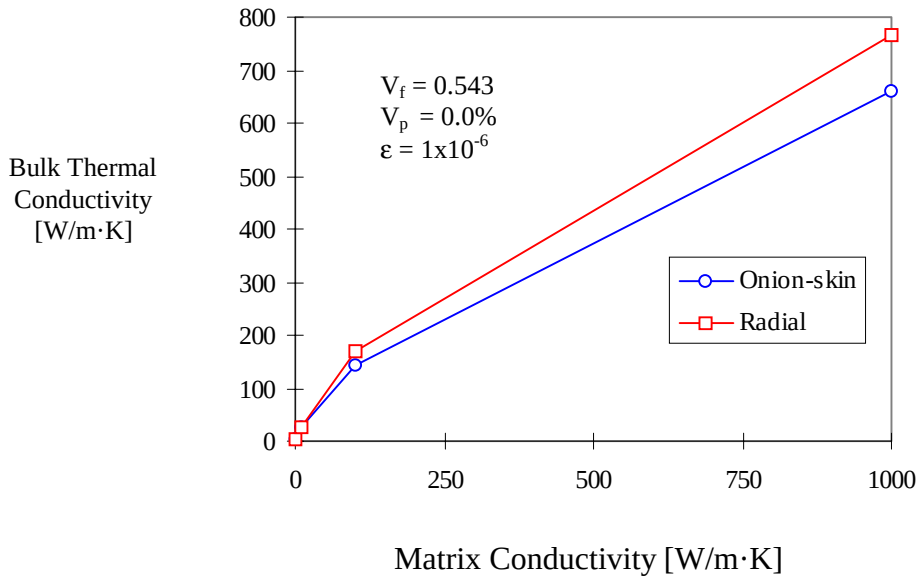

Figure 8. Thermal conductivity of a microscopic section with radial and onion skin fibers.

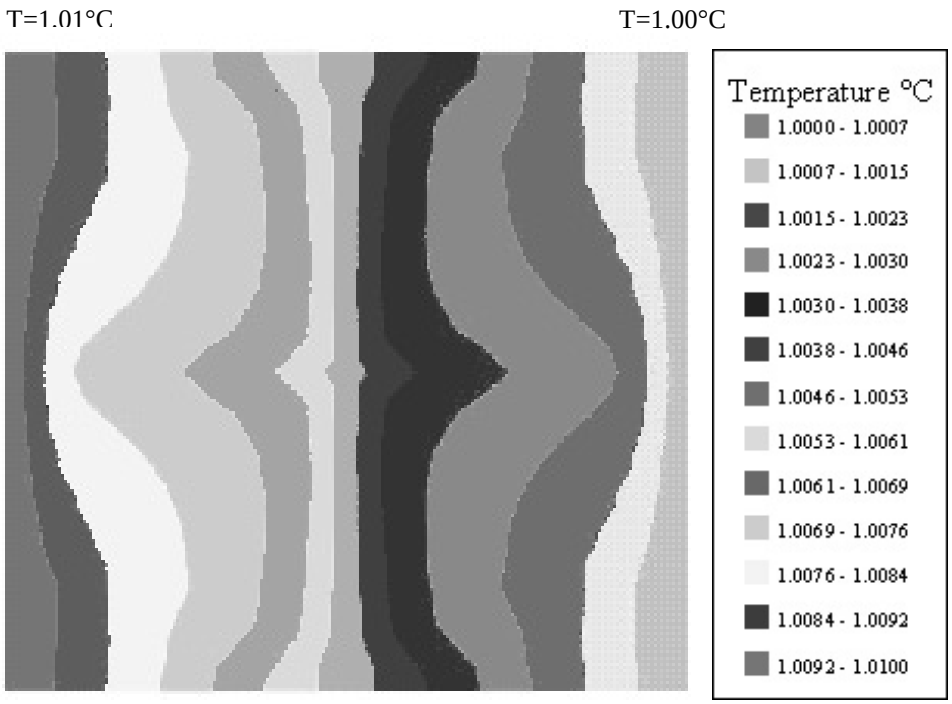

(a)

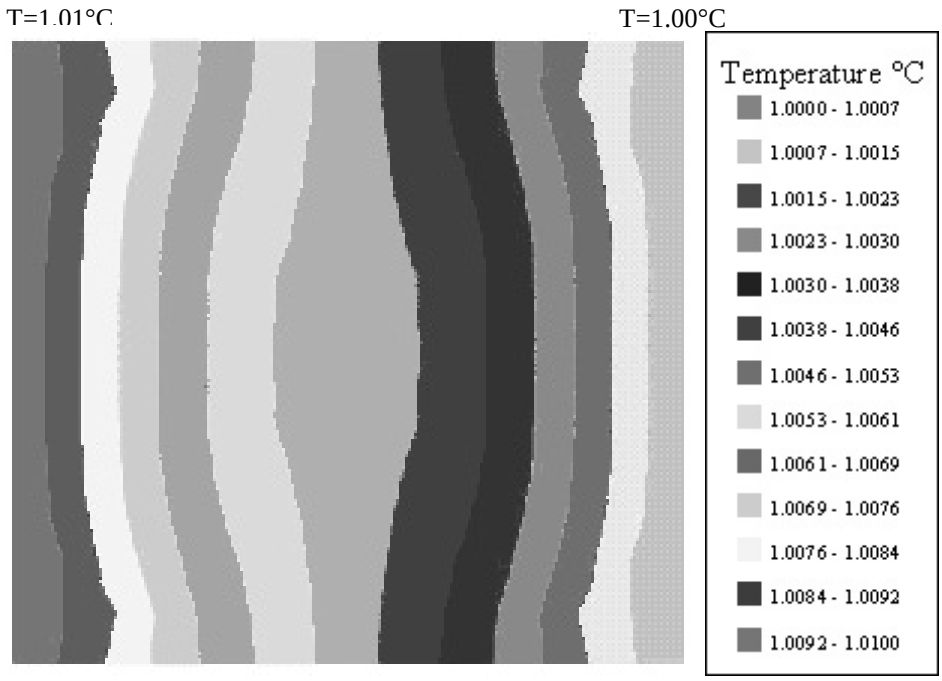

(b)

Figure 9. Temperature profile in a composite with (a) a radial fiber and (b) an onion skin fiber.

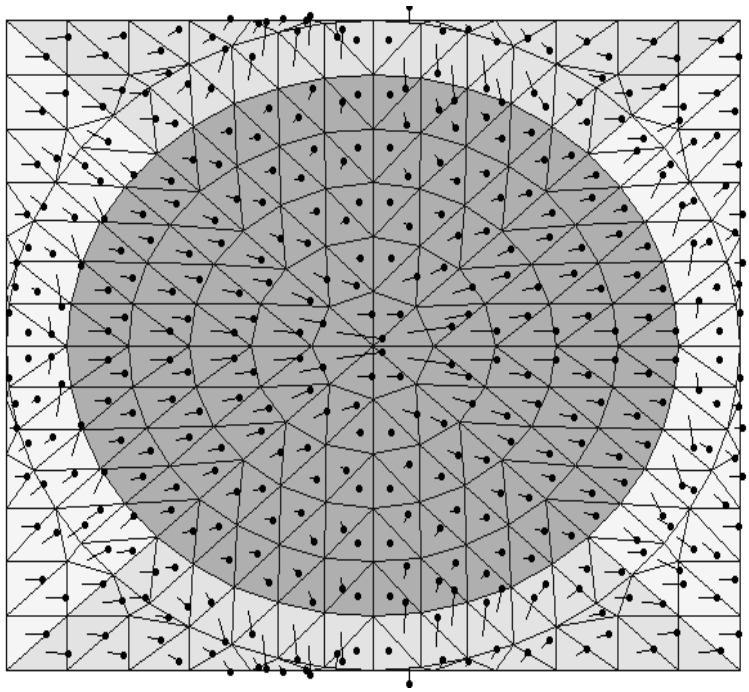

(a)

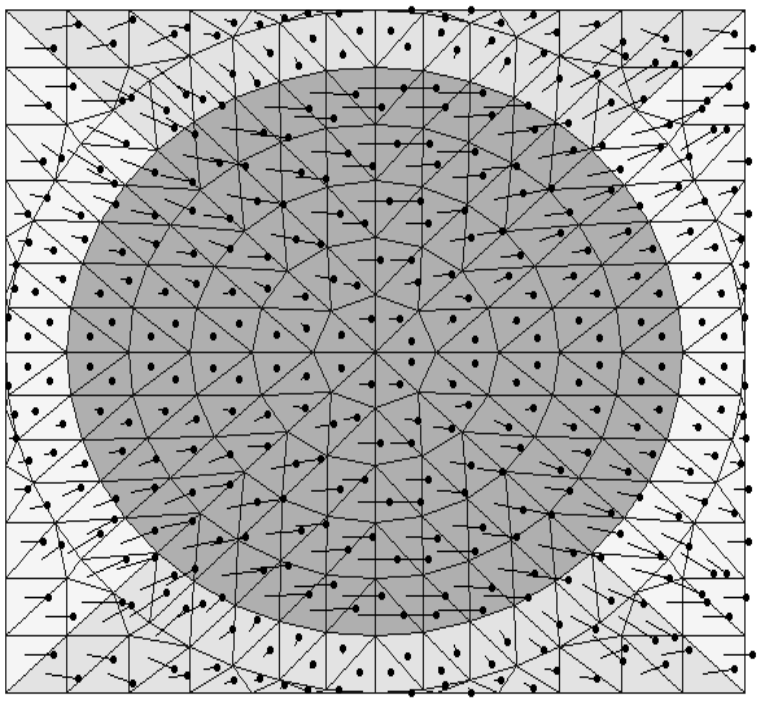

(b)

Figure 10. Map of fluxes in a composite with (a) a radial fiber and (b) an onion skin fiber.

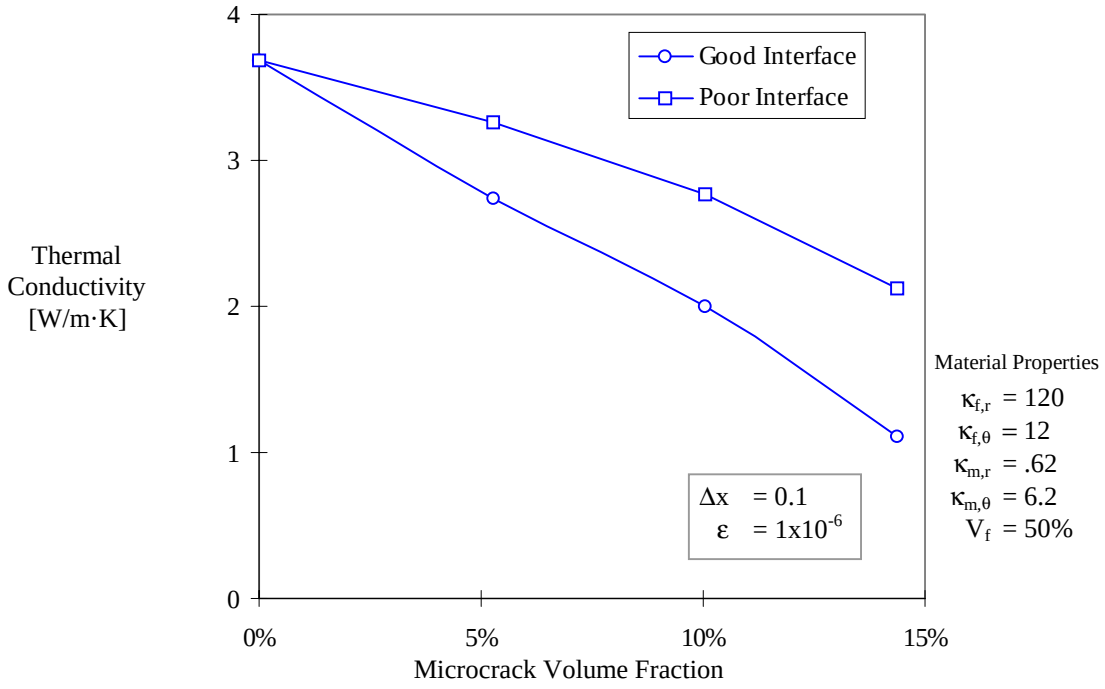

Figure 11. Thermal conductivity of a composite section, transverse to the fibers, with good and poor fiber/matrix interfaces.

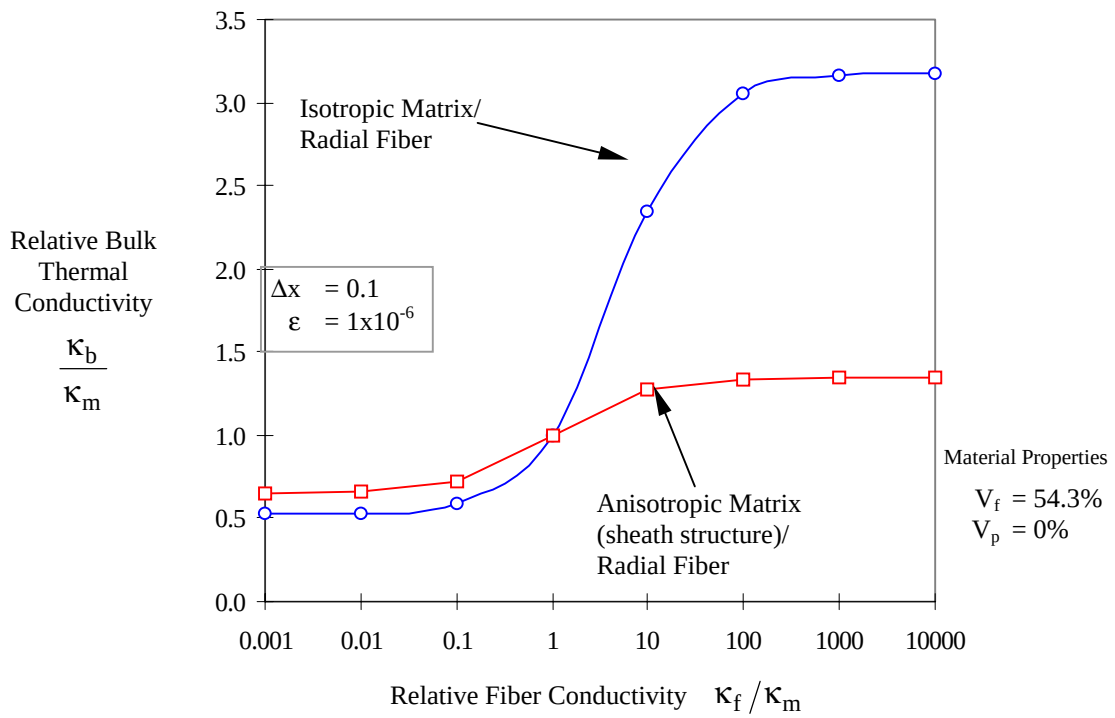

Figure 12. Plot of bulk composite transverse thermal conductivity versus transverse fiber conductivity relative to the matrix conductivity.